WILEY InterScience® DISCOVER SOMETHING GREAT

PROTEINS STRUCTURE ■ FUNCTION ■ BIOINFORMATICS

STRUCTURE NOTE

Crystal structure of ACE19, the collagen binding subdomain of *Enterococus Faecalis* surface protein ACE

Karthe Ponnuraj and Sthanam V.L. Narayana*

School of Optometry and Center for Biophysical Sciences and Engineering, University of Alabama at Birmingham, Birmingham, Alabama 35294

INTRODUCTION

Enterococus faecalis is an extracellular pathogen known to cause many clinical infections, such as septicemia, bacteremia, and urinary tract infections.[1] The bacterial pathogenesis is a complex process at the molecular level and the bacterial adherence to extracellular matrix components like collagen, fibrinogen, and fibronectin is a prerequisite for pathogenesis. Gram-positive bacteria are endowed with adhesive proteins termed as MSCRAMMs (Microbial Surface Component Recognizing Adhesive Matrix Molecules), located on the surface of the microbe to mediate such attachment. Characterization of several MSCRAMMs from various bacterial species revealed that they are structurally similar.[2] In general, they contain an N-terminal signal peptide followed by (i) a ligand binding A region that is composed of two or more subdomains, each adopting a novel immunoglobulin-like (DEv-IgG) fold[3]; (ii) a B region that is made up of short repeat sequences; and (iii) the C-terminal end that contains the cell wall anchoring LPXTG motif, a hydrophobic transmembrane region (M), and a positively charged cytoplasmic tail (c), features that are essential for sorting these proteins to the cell wall.[2]

ACE is a collagen binding MSCRAMM of *E. faecalis*.[4,5] The structural characteristics of ACE are similar to that of collagen binding protein CNA of *Staphylococcus aureus* [Fig. 1(A)], which has been studied in significant detail both in structural and biochemical aspects.[6–10] The 55-kDa ligand binding A region of CNA (termed CNA55) contains three subdomains namely N_1, N_2, and N_3 and the minimum collagen binding region was localized to a 19-kDa N2 subdomain (termed CNA19) and its crystal structure was solved earlier in our laboratory.[8] Recently, we determined the crystal structure of N_1N_2 subdomain of CNA (termed CNA35) both as an apo-protein and in complex with a synthetic collagen triple helix peptide. On the basis of these two crystal structures, we proposed a "Collagen Hug" binding mechanism for the association of CNA with collagen.[11] The crystal structure of CNA35-collagen complex revealed that collagen-like triple helical peptide mainly interacts with residues present in the "trench" region of the N2 domain, however, N1 domain also contributes critical residues for the stabilization of complex by sequestering critical regions of the ligand, explaining the 10-fold higher ligand binding affinity of CNA35 (N1 and N2) compared with CNA19.

The 40-kDa A-region of ACE (termed ACE40) was predicted to have two subdomains namely N1 and N2. CNA55 and ACE40 share significant sequence similarity and particularly the minimum ligand binding region of CNA (CNA19) exhibits high degree of similarity (about 95%) with the corresponding region of ACE40 (i.e. ACE19). Previous modeling and spectroscopic studies predicted that the backbone folding of ACE19 is highly

Karthe Ponnuraj's current address is: Department of Crystallography and Biophysics, University of Madras, Guindy Campus, Chennai–600 025, India.
*Correspondence to: Sthanam V.L. Narayana, Center for Biophysical Sciences and Engineering, University of Alabama at Birmingham, Birmingham, AL 35294.
E-mail: narayana@cbse.uab.edu
Received 22 December 2006; Revised 18 January 2007; Accepted 29 January 2007
Published online 7 June 2007 in Wiley InterScience (www.interscience.wiley. com).
DOI: 10.1002/prot.21464

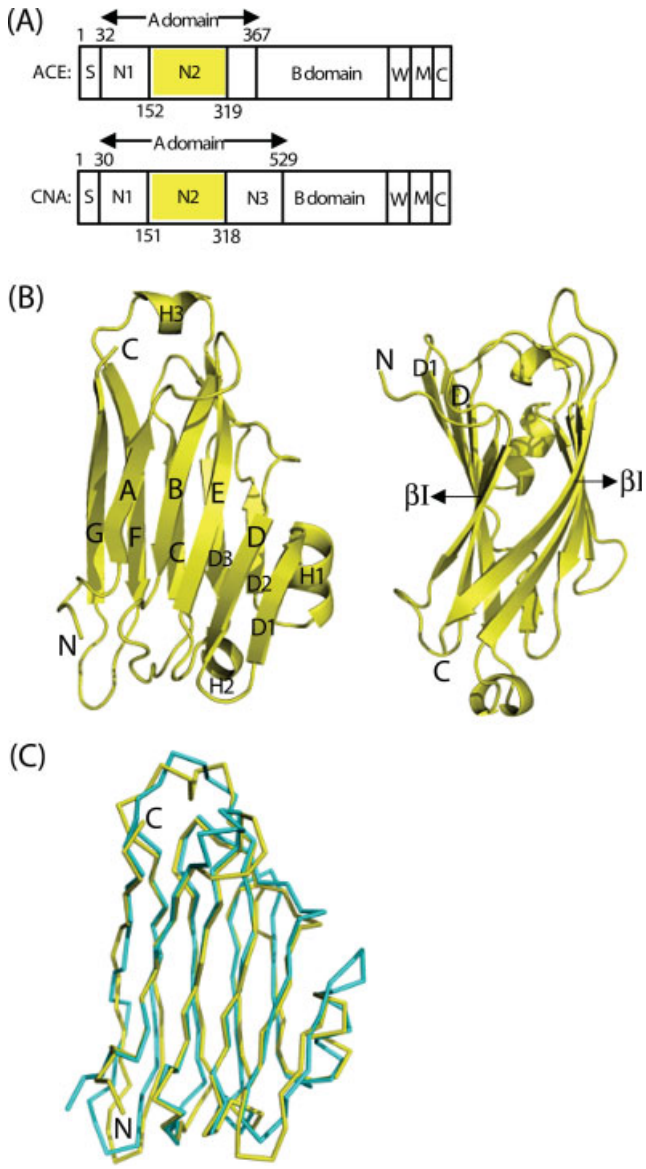

Figure 1

*(**A**) Domain organization of* E. faecalis *ACE and* S. aureus *CNA. Both MSCRAMMS have a N-terminal signal peptide, a collagen-binding domain (A), a region of repeat units (B), a cell wall-anchoring domain (W), a membrane-spanning domain (M) and a positively charged C-terminal domain (C). The 19 kDa subdomain (N2) in both ACE and CNA is indicated in yellow and the present paper reports the crystal of structure of that region of ACE. (**B**) Ribbon representation of crystal structure of ACE19 in two different views. Strands A, B, E, D, and D1 form β-sheet I (βI), strands D2, D3, C, F and G form β-sheet II (βII). The putative collagen-binding trench region formed by the βI is indicated. (**C**). (**C**) Backbone superposition of crystal structures of ACE19 (yellow) and CNA19 (cyan) showing very identical fold.*

similar to that of CNA19. However, the kinetic studies suggest the mechanism of collagen binding to be significantly distinct between CNA and ACE.[4] The first observation is that the ACE40 associates and disassociates with collagen rapidly whereas CNA55 does slowly. The second observation is CNA55 and CNA19 interacts with collagen at a greater number of sites with varying affinities. In contrast, ACE40 interacts with collagen at less number of sites, but with equal affinities, whereas ACE19 exhibits very littlie affinity to collagen. These observations suggest that two homologous MSCRAMM proteins, from two different pathogens, interact with a common host molecule collagen in different modes.

We initiated X-ray crystallographic studies on ACE19 and ACE40 to gain further insights into the collagen recognition by *E. faecalis* ACE, as well as to address some specific questions like (1) what accounts for ACE and CNA's different affinities for collagen? (2) Which of the critical residues in ACE are involved in collagen binding? (3) Which additional regions of A-domain influence the ACE association with collagen, if not the trench region of ACE19 N2? Here we describe the crystal structure of ACE19 and compare it with CNA19 crystal structure. In addition, we present modeling studies to localize the collagen-like peptide interactions with ACE19.

MATERIALS AND METHODS

Procedures for the purification, crystallization, and data collection of ACE19 have been previously published.[12] Briefly, ACE19 protein was expressed and purified by Ni^{2+} charged HiTrap chelating column as described by Rich et al.[4] Single crystals of ACE19 were obtained in two different crystal forms such as trigonal and orthorhombic as reported by Ponnuraj et al.[12] Structural analysis was carried out with orthorhombic crystals since they diffracted to at least 1.6 Å whereas the trigonal crystals diffracted to only 2.8 Å.

The structure of ACE19 was solved by MIR (Multiple Isomorphous Replacement) method since the attempts to find a molecular replacement solution using the model of CNA19 were unsuccessful. MIR solution was found based on the Palladium, Uranyl and Platinum derivatives using the program SOLVE.[13] Density modification using the program DM[14] was used to improve the phases obtained from SOLVE. The overall figure of merit of the initial experimental phases calculated to 2.5 Å was 0.53 and 0.70 after density modification. The solvent-flattened map allowed the tracing of >80% of the model, using QUANTA2000 (Molecular Simulations). The structure was subsequently refined with CNS[15] using a high-resolution data at 1.65 Å resolution. The final crystallographic R and R_{free} were 19.8% and 21.6%, respectively. The protein model and accounts for all 146-residues of the expressed protein, 180 water molecules and 2 sulfate ions, which we believe, comes from the ammonium sulfate used in the crystallization solution. In a Ramachandran plot of ACE19 calculated with PROCHECK[16] 97.1% of the residues lie in the most favored regions, 2.9% in additionally allowed regions. Final refinement statistics are listed in Table 1.

DOI 10.1002/prot

Table I
Crystallographic and Refinement Data of ACE19

	ACE19
Crystal data	
a (Å)	38.43
b (Å)	48.91
c (Å)	83.73
$\alpha = \beta = \gamma$ (degree)	90
Space group	$P2_12_12_1$
Resolution (Å)	50–1.65
Reflections total/unique	194,455/19,670
Completeness (%)	99.9
R_{sym}	4.6
No of molecules in the asymmetric unit	1
Refinement	
Resolution range	20–1.65
R_{cryst}/R_{free} (%) (All data with 0 sigma cutoff)	0.198/0.216
Average B value (Å^2)	15.9
Rmsd for bonds (Å)	0.006
Rmsd for angles (degree)	1.356
No of nonhydrogen protein atoms	1187
No of water molecules	188
No of ions	2
PDB ID	2OKM

Structure figures were generated with PyMOL (http://www.pymol.org). Superpositions of the structures were accomplished using the program TOP.[17]

RESULTS AND DISCUSSION

The structure of ACE19 is shown in Figure 1(B). ACE19 folds into a compact, slightly elongated domain composed of two principal β-sheets βI and βII. Both sheets consist of five antiparallel β-strands that stack face-to-face and form "β-sandwich" with DEv-IgG (DEvarient-IgG) fold.[3] βI is composed of strands A, B, E, D, and D1 and βII contains strands D2, D3, C, F, and G. βI and βII are connected by a helix at one end of the molecule such that strand D1 of βI, helix H1 and strand D2 of βII form a β-α-β motif.

The crystal structure of ACE19 exhibits a prominent groove on the βI sheet indicating the putative collagen-binding region [Fig. 1(B)]. In a recently solved crystal structure of CNA35-collagen complex,[11] the collagen peptide nicely fits into such groove present on N2 domain of CNA35 (equivalent to that of ACE19) and interacts with residues present in the trench. In ACE19, the corresponding trench region is made up of 32-residues including 9 nonpolar, 15 polar, and 8 charged residues.

The comparison of ACE19 and CNA19 crystal structures revealed similar topology with analogous collagen-binding trench regions [Fig. 1(C)]. The rms deviation for the main chain atoms between the two structures is 1.3 Å. Although the structure and topology of βI sheet that forms the collagen binding trench in ACE19 and CNA19 is very similar, their surface properties are significantly different. For example ACE19 displays 3 arginines, 1 lysine, 3 asparagines, and 4 threonines on its βI sheet, CNA19 contains 1 arginine, 3 lysines, 5 asparagines, and 7 threonines. To find out what extent these variations in the surface charges in the trench region influences the binding of collagen in CNA19 and ACE19, we performed docking studies using collagen peptide as a probe and the crystal structures of CNA19 and ACE19 as receptors with the help of GRAMM[18] program. The coordinates of collagen motif [(GPO)4GPRGRT[(GPO)4] obtained from the CNA35-collagen complex structure were truncated to [(GPO)2GPRGRT[(GPO)2] and used in these docking studies. As expected, the trench region on βI sheet of CNA19 was predicted as the ligand binding site [Fig. 2(A)] that coincides with the ligand binding region and direction observed in the crystal structure of CNA35-collagen complex [Fig. 2(B)]. In contrast, the collagen probe was positioned at one end of the βI sheet of ACE19 such that it stacked against the β-strands D and D1. In this orientation the collagen's triple helical axis is almost parallel with the strands D and D1 [Fig. 2(C)], a different position and orientation in trench compared to CNA19 and CNA35-collagen complex. In later structures the triple helical axis of the collagen is orientated perpendicular to the strands of βI sheet. Thus docking studies of ACE19 and CNA19 indicate that they bind collagen probes differently, although the overall structure of βI sheet is conserved between the two structures. These observations, nevertheless confirmative, could possibly explain the dramatic difference in the binding affinities towards the collagen peptide. CNA19 binds collagen with an apparent dissociation constant (K_D) of 36 μ*M*,[8] whereas ACE19 binds collagen with very low affinity (data not shown).

Structural comparison also reveal significant differences and in trench residue compositions, especially around Arg174, Tyr176, Tyr238, and Arg277 of ACE19 [Fig. 2(D)]. The first two residues, located at the tip of the N2 domain N-terminus are small residues such as Thr169 and Ser171, respectively in CNA19. The side chains of both Arg174 and Tyr176 are projected into the trench of ACE19, spatially occupying the one end of the trench. The third variant residue Tyr238 of ACE19 is located at the other end, however the corresponding tyrosine (Tyr233) in the trench of CNA19 is orientation is in different orientation. In CNA19 the side chain of Tyr233 points upwards, with its aromatic ring parallel to the trench wall, whereas Tyr238 in ACE19 is directed towards the middle of the trench [Fig. 2(D)]. Similarly Arg277 of ACE19 is also projected towards the middle of the groove [Fig. 2(D)] similar to its equivalent residue Asn278 in CNA19. Tyr238 and Arg277 of ACE19 are spatially close to one another and therefore create a local bump projected into the groove, thus presenting a shallow part of the trench. It is most likely that these four residues (Arg174, Tyr176, Tyr238, and Arg277), projected

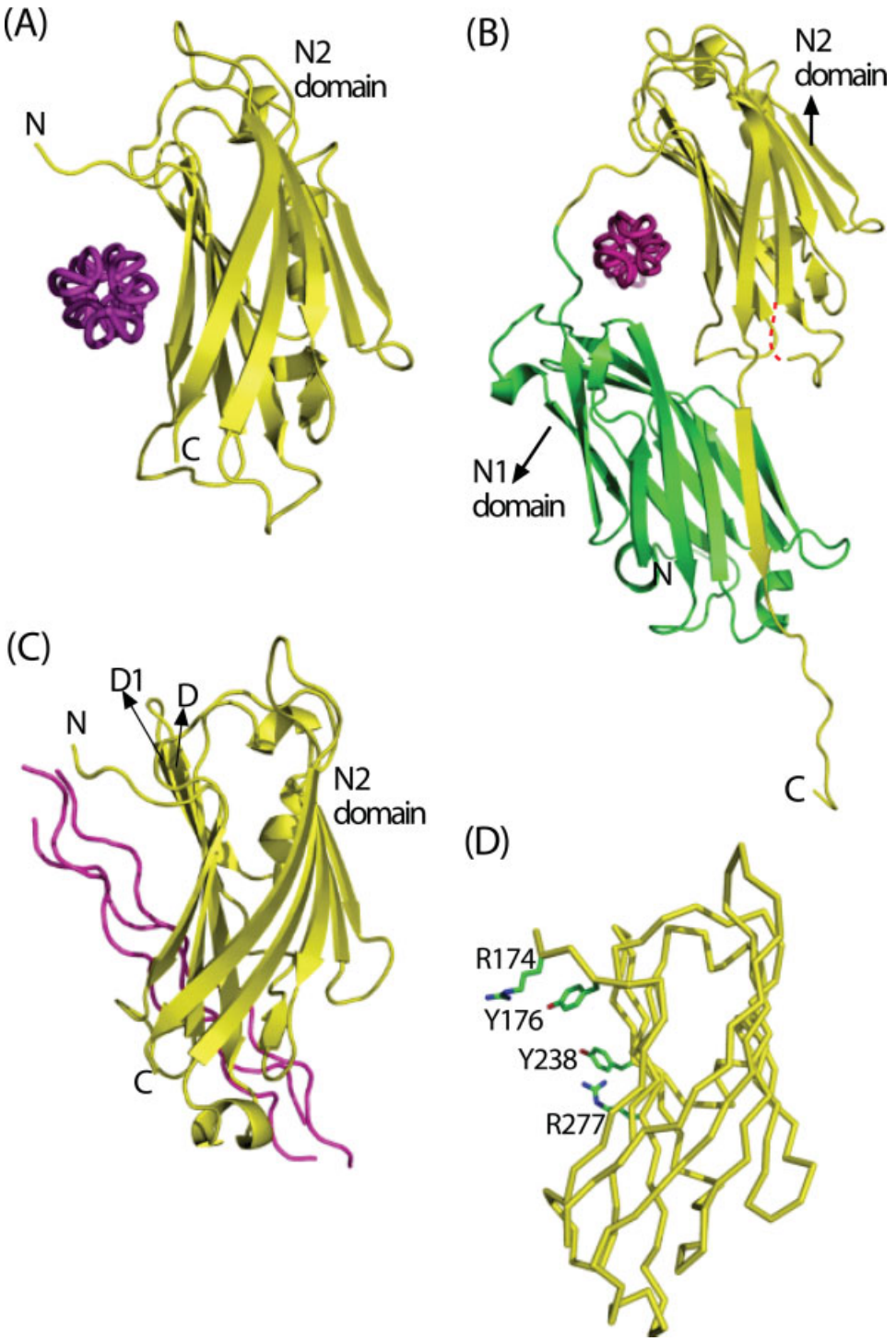

Figure 2

*(**A**) Docking of collagen peptide (pink) with the crystal structure of CNA19. The ligand is oriented in such a way that its triple helical axis is perpendicular to the strands of βI. (**B**) Ribbon representation of crystal structure of CNA35-collagen complex. The ligand is positioned inside a hole formed by the two subdomains (N1 and N2) and a linker that connects N1 and N2. The ligand mainly interacts with residues in the trench of the N2 domain. (**C**) Crystal structure of ACE19 docked with collagen peptide. The ligand is positioned at one end of the trench with its helical axis parallel to the strands (D and D1) of βI. (**D**) Backbone structure of ACE19 with four residues that are significantly different in comparison with surface residues of βI of CNA19. Projection of these four residues in ACE19 reduces the shallowness of the trench.*

DOI 10.1002/prot

out from the surface of βI sheet of ACE19, are responsible for low binding affinity towards the collagen peptide.

To validate this conclusion, the above four residues were mutated and modeled into alanines and the docking studies were repeated. A dramatic difference in docking position was observed. The ligand positions in the trench with an orientation similar to the one observed in both CNA35-collagen complex and CNA19 docked with collagen probe.

The crystal structure of ACE19 and subsequent docking studies thus provided plausible explanation for its contrasting behavior in binding to collagen when compared with CNA19. The crystal structure of ACE40 and further mutational analysis will provide additional insights into the collagen binding mechanism of this MSCRAMM.

REFERENCES

1. Murray BE. The life and times of the *Enterococcus*. Clin Microbiol Rev 1990;3:46–65.
2. Patti JM, Allen BL, McGavin MJ, Hook M. MSCRAMM-medicated adherence of microorganisms to host tissues. Annu Rev Microbiol 1994;48:585–617.
3. Deivanayagam CCS, Wann ER, Chen W, Carson M, Rajashankar KR, Hook M, Narayana SVL. A novel variant of the immunoglobulin fold in surface adhesins of *Staphylococcus aureus*: crystal structure of the fibrinogen-binding MSCRAMM, clumping factor A. EMBO J 2002;27:6660–6672.
4. Rich RL, Kreikemeyer B, Owens RT, LaBrenz S, Narayana SVL, Weinstock GM, Murray BE, Hook M. Ace is a collagen-binding MSCRAMM from *Enterococcus faecalis*. J Biol Chem 1999;274: 26939–26945.
5. Nallapareddy SR, Qin X, Weinstock GM, Hook M, Murray BE. *Enterococcus faecalis* adhesin, ace, mediates attachment to extracellular matrix proteins collagen type IV and laminin as well as collagen type I. Infect Immun 2000;68:5218–5224.
6. Patti JM, Boles JO, Hook M. Identification and biochemical characterization of the ligand binding domain of the collagen adhesin from *Staphylococcus aureus*. Biochemistry 1993;32:11428–11435.
7. Patti JM, House-Pompeo K, Boles JO, Garza N, Gurusiddappa S, Hook M. Critical residues in the ligand-binding site of the *Staphylococcus aureus* collagen-binding adhesin (MSCRAMM). J Biol Chem 1995;270:12005–12011.
8. Symersky J, Patti JM, Carson M, House-Pompeo K, Teale M, Moore D, Jin L, DeLucas LJ, Hook M, Narayana SVL. Structure of the collagen-binding domain from *Staphylococcus aureus* adhesin. Nat Struct Biol 1997;10:833–838.
9. Visai L, Xu Y, Casolini F, Rindi S, Hook M, Speziale P. Monoclonal antibodies to CNA, a collagen-binding microbial surface component recognizing adhesive matrix molecules, detach *Staphylococcus aureus* from a collagen substrate. J Biol Chem 2000;275: 39837–38945.
10. Deivanayagam CCS, Rich RL, Carson M, Owens RT, Danthuluri S, Bice T, Hook M, Narayana SVL. Novel fold and assembly of the repetitive B region of the *Staphylococcus aureus* collagen-binding surface protein. Structure 2000;8:67–78.
11. Zong Y, Xu Y, Liang X, Keene DR, Hook A, Gurusiddappa S, Hook M, Narayana SV. A 'Collagen Hug' model for *Staphylococcus aureus* CNA binding to collagen. EMBO J 2005;24:4224–4236.
12. Ponnuraj K, Xu Y, Moore D, Deivanayagam CCS, Boque L, Hook M, Narayana SVL. Crystallization and preliminary X-ray crystallographic analysis of Ace: a collagen-binding MSCRAMM from *Enterococcus faecalis*. Biochem Biophys Acta 2002;1596:173–176.
13. Terwilliger TC, Berendzen J. Automated structure solution for MIR and MAD. Acta Crystallogr D Biol Crystallogr 1999;55:849–861.
14. Cowton K. DM an automated procedure for phase improvement by density modification. In: Bailey S, Wilson K, editors. Joint CCP4 and ESF-EACBM newsletter on protein crystallography, Vol. 31. Warrington, UK: SERC Daresbury Laboratory; 1994. pp 34–38.
15. Brünger AT, Adams PD, Clore GM, DeLano WL, Gros P, Grosse-Kunstleve RW, Jiang JS, Kuszewski J, Nilges M, Pannu NS, Read RJ, Rice LM, Simonson T, Warren GL. Crystallographic and NMR system: a new software system for macromolecular structure determination. Acta Crystallogr D 1998;50:760–763.
16. Laskowski RA, Macarthur MW, Moss DS, Thornton JM. PROCHECK: a program to check the stereochemical quality of the protein structures. J Appl Cryst 1993;26:283–291.
17. Lu G. TOP: a new method for protein structure comparisons and similarity searches. J Appl Crystallogr 2000;33:176–183.
18. Katchalski-Katzir E, Shariv I, Eisenstein M, Friesem AA, Aflalo C, Vakser IA. Molecular surface recognition: determination of geometric fit between proteins and their ligands by correlation techniques. Proc Natl Acad Sci USA 1992;89:2195–2199.